http://doi.org/10.35784/iapgos.6141 *received: 24.04.2024 | revised: 27.04.2024 | accepted: 04.09.2023 | available online: 30.09.2024*

POLARIZATION-CORRELATION MAPPING OF MICROSCOPIC IMAGES OF BIOLOGICAL TISSUES OF DIFFERENT MORPHOLOGICAL STRUCTURE

Nataliia Kozan[1], Oleksandr Saleha[2], Olexander Dubolazov[2], Yuriy Ushenko[2], Irina Soltys[2], Oleksandr Ushenko[2], Oleksandr Olar[2], Victor Paliy[3], Saule Smailova[4]

[1] Ivano-Frankivsk National Medical Academy, Ivano-Frankivsk, Ukraine, [2]Yuriy Fedkovych Chernivtsi National University, Chernivtsi, Ukraine, [3]National Pirogov Memorial University of Vinnytsia, Ukraaine, [4]D.Serikbayev East Kazakhstan State Technical University, Ust-Kamenogorsk, Kazakhstan

Abstract. *The results of polarization-correlation mapping of the fourth parameter of the two-point Stokes vector of microscopic images of histological sections of biological tissues with different architectonics of the optically anisotropic polycrystalline component are presented. The coordinate distributions of randomly generated values representing the modulus of the fourth parameter of the polarization-correlation vector from microscopic images of histological sections of fibrillar tissues (such as skin dermis) and parenchymal tissues (like spleen) have been replicated. The statistical analysis results of algorithmically generated coordinate distributions of random values representing the modulus of the fourth parameter of the polarization-correlation vector from microscopic images of histological sections of biological tissues with varying morphological structures are provided.*

Keywords: polarization, correlation, Stokes vector, statistical analysis, biological tissues

MAPOWANIE POLARYZACYJNO-KORELACYJNE OBRAZÓW MIKROSKOPOWYCH TKANEK BIOLOGICZNYCH O RÓŻNEJ STRUKTURZE MORFOLOGICZNEJ

Streszczenie. *Przedstawiono wyniki mapowania polaryzacyjno-korelacyjnego czwartego parametru dwupunktowego wektora Stokesa z obrazów mikroskopowych przekrojów histologicznych tkanek biologicznych o różnej architekturze optycznie anizotropowego składnika polikrystalicznego. Odtworzono rozkłady współrzędnych losowo generowanych wartości reprezentujących moduł czwartego parametru wektora korelacji polaryzacji z obrazów mikroskopowych przekrojów histologicznych tkanek włóknistych (takich jak skóra właściwa) i tkanek miąższowych (takich jak śledziona). Przedstawiono wyniki analizy statystycznej algorytmicznie wygenerowanych rozkładów współrzędnych losowych wartości reprezentujących moduł czwartego parametru wektora korelacji polaryzacji z obrazów mikroskopowych przekrojów histologicznych tkanek biologicznych o różnej strukturze morfologicznej.*

Słowa kluczowe: polaryzacja, korelacja, wektor Stokesa, analiza statystyczna, tkanki biologiczne

Introduction

Laser polarimetry techniques have gained extensive use in diagnosing the optically anisotropic characteristics of morphological structures within biological tissues and liquids [1–3]. Currently, a wide class of optical-electronic devices has been created for the instrumental implementation of such polarimetric techniques [4, 5, 7]. Using the latest methods of polarization Stokes parametric mapping, diagnostically relevant relationships between polarization maps of azimuth and polarization ellipticity and statistical moments of 1-4 orders are determined [1, 6, 8]. As a result, the possibility of successful diagnosis of pathological (cancer) and necrotic (time of death) conditions of biological tissues was demonstrated [9, 10, 13].

At the same time, such methods do not provide information about the correlation structure of polarization maps of biological objects. There is a small number of publications devoted to the correlometry of polarization images [11, 14]. However, such information can be decisive in improving the sensitivity of laser polarimetry methods [12, 15, 16].

Our research focuses on investigating the polarization-correlation patterns within laser fields of histological sections from biological tissues with varying morphological structures. We aim to identify the most sensitive diagnostic markers by statistically analyzing the coordinate distributions of the modulus of two-point parameters of the Stokes vector [15].

1. Two-point parameters of the Stokes vector

For the analytical description of the spatial correlation structure of stationary distributions of random values of complex amplitude values of laser object fields of optically anisotropic biological layers, a matrix of mutual spectral density is used, which has the following form

$$W_{i,j}(p_1,p_2) = E_i^*(p_1)\cdot E_j(p_2), i,j = x,y \tag{1}$$

By applying the given matrix operator, the following analytical expressions were introduced for the set of "two-point" parameters of the Stokes vector

$$S_0 = W_{xx}(p,p_2) + W_{yy}(p_1,p_2) \tag{2}$$

$$S_1 = W_{xx}(p_1,p_2) - W_{yy}(p_1,p_2) \tag{3}$$

$$S_2 = W_{xy}(p,p_2) + W_{yx}(p_1,p_2) \tag{4}$$

$$S_3 = i\left[W_{yx}(p_1,p_2) - W_{xy}(p_1,p_2)\right] \tag{5}$$

where

$$\begin{cases} W_{xx}(p_1,p_2) = E_x^*(p_1)E_x(p_2) \\ W_{yy}(p_1,p_2) = E_y^*(p_1)E_y(p_2) \\ W_{xy}(p_1,p_2) = E_x^*(p_1)E_y(p_2) \\ W_{yx}(p_1,p_2) = E_y^*(p_1)E_x(p_2) \end{cases} \tag{6}$$

here $E_x^*(p_1), E_x(p_2)$ and $E_y^*(p_1)E_y(p_2)$ – orthogonal components of amplitude E in neighbors $(p_1\ and\ p_2)$ points of object field; "$*$" – notation of complex conjugation operation.

2. Laser polarization – correlometry optical technique

The optical and functional block diagram of laser polarimetry, used in numerous studies [13] of biological layers, is shown in Fig. 1.

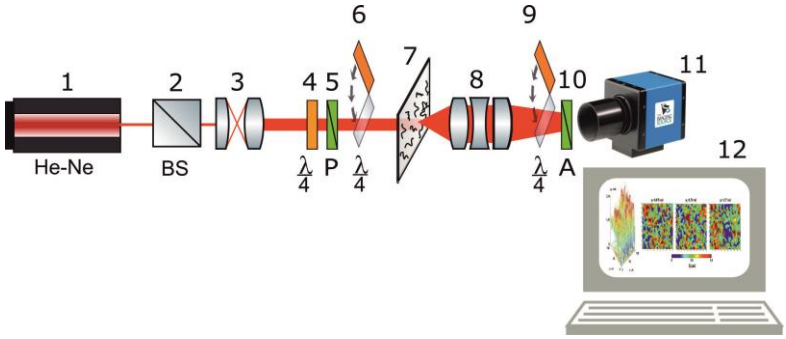

Fig. 1. Optical and functional block diagram of the polarimeter, where 1 – He-Ne laser; 2,3 – collimator; 4 – quarter-wave stationary plate; 6, 9 – mechanically moving quarter-wave plates; 5, 10 – analyzer and polarizer; 7 – biological layer; 8 – microlens polarizing; 11 – CCD camera; 12 –computer

3. The method of polarization mapping of the polarization-correlation vector

The experimental method for Stokes correlometry mapping of the biological layer's object field involves the following series of procedural steps. By applying two-dimensional discrete Fourier transforms, distributions of complex amplitudes of the object field are reproduced.

Using a series of the following analytical ratios, the parameters of the polarization-correlation vector are calculated

$$S_1^{12} = A_{11} + iB_{11} \quad (7)$$

$$A_{11} = E_{x1}E_{x2}\cos(\Theta_{x2} - \Theta_{x1}) - E_{y1}E_{y2}\cos(\Theta_{y2} - \Theta_{y1}) \quad (8)$$

$$B_{11} = E_{x1}E_{x2}\sin(\Theta_{x2} - \Theta_{x1}) - E_{y1}E_{y2}\sin(\Theta_{y2} - \Theta_{y1}) \quad (9)$$

$$|S_1^{12}| = \sqrt{A_{11}^2 + B_{11}^2} \quad (10)$$

$$\mathrm{Arg}S_1^{12} = arctg\left(\frac{B_{11}}{A_{11}}\right) \quad (11)$$

$$S_2^{12} = A_{22} + iB_{22} \quad (12)$$

$$A_{22} = E_{x1}E_{x2}\cos(\Theta_{x2} - \Theta_{x1}) - E_{y1}E_{y2}\cos(\Theta_{y2} - \Theta_{y1}) \quad (13)$$

$$B_{22} = E_{x1}E_{x2}\sin(\Theta_{x2} - \Theta_{x1}) - E_{y1}E_{y2}\sin(\Theta_{y2} - \Theta_{y1}) \quad (14)$$

$$|S_2^{12}| = \sqrt{A_{22}^2 + B_{22}^2} \quad (15)$$

$$\mathrm{Arg}S_2^{12} = arctg\left(\frac{B_{22}}{A_{22}}\right) \quad (16)$$

$$S_3^{12} = A_{33} + iB_{33} \quad (17)$$

$$A_{33} = E_{x1}E_{y2}\cos(\Theta_{y2} - \Theta_{x1}) - E_{y1}E_{x2}\cos(\Theta_{x2} - \Theta_{y1}) \quad (18)$$

$$B_{33} = E_{x1}E_{y2}\sin(\Theta_{y2} - \Theta_{x1}) - E_{y1}E_{x2}\sin(\Theta_{x2} - \Theta_{y1}) \quad (19)$$

$$|S_3^{12}| = \sqrt{A_{33}^2 + B_{33}^2} \quad (20)$$

$$\mathrm{Arg}S_3^{12} = arctg\left(\frac{B_{33}}{A_{33}}\right) \quad (21)$$

$$S_4^{12} = Q + iF \quad (22)$$

$$A_{44} = E_{y1}E_{x2}\cos(\Theta_{x2} - \Theta_{y1}) - E_{x1}E_{y2}\cos(\Theta_{y2} - \Theta_{x1}) \quad (23)$$

$$B_{44} = E_{y1}E_{x2}\sin(\Theta_{x2} - \Theta_{y1}) - E_{x1}E_{y2}\sin(\Theta_{y2} - \Theta_{x1}) \quad (24)$$

$$|S_4^{12}| = \sqrt{A_{44}^2 + B_{44}^2} \quad (25)$$

$$\mathrm{Arg}S_4^{12} = arctg\left(\frac{B_{44}}{A_{44}}\right) \quad (26)$$

The technique for measuring two-point parameters of the Stokes vector is given in detail in [1]. Here, for better comprehension of the experimental data, we offer only concise theoretical details regarding the measured magnitude of the fourth parameter of the Stokes vector $|S_4^{12}|$ in microscopic images of histological sections of biological tissues.

$$|S_4^{12}| = \sqrt{A_{44}^2 + B_{44}^2}; \quad (27)$$

$$A_{44} = E_{y1}E_{x2}\cos(\Theta_{x2} - \Theta_{y1}) - E_{x1}E_{y2}\cos(\Theta_{y2} - \Theta_{x1}) \quad (28)$$

$$B_{44} = E_{y1}E_{x2}\sin(\Theta_{x2} - \Theta_{y1}) - E_{x1}E_{y2}\sin(\Theta_{y2} - \Theta_{x1}) \quad (29)$$

here $E_{y1}; E_{x2}$ i $E_{x1}; E_{y2}$ – orthogonal components of the complex amplitude of laser radiation are the distinct aspects of the laser light's complex wave properties, observed at different points within a digital microscopic image of histological sections of biological tissues; $\Theta_{x1,x2}$; and $\Theta_{y1,y2}$ – phase angles.

4. The arrangement and statistical characteristics of polarization-correlation maps specific to the skin dermis

We investigated the variation in parameters within polarization-correlation maps, specifically focusing on the modulus of the fourth parameter of the polarization-correlation vector in microscopic images of histological sections of skin dermis. This exploration encompassed different polarization states of the incident laser beam, including linearly polarized states with specified azimuths $0^0; 90^0; 45^0$.

In a series of fragments of Fig. 2 presents the results of polarization-correlation mapping of microscopic images of histological sections of the dermis of the skin (a representative sampling of 23 samples) of people who died as a result of myocardial infarction.

Analysis of the results of polarization-correlation mapping of the modulus of the fourth parameter of the polarization-correlation vector S_4^{12} microscopic images of histological sections of the skin dermis revealed:

- All layered polarization-correlation maps of the modulus of the fourth parameter $|S_4^{12}|(m \times n)$ the two-point Stokes vector parameters within a microscopic image of a histological section of skin dermis exhibit both coordinate and topographical heterogeneity – Fig. 2 – fragments (1)–(3).
- Histograms of distributions of the modulus of the fourth parameter $|S_4^{12}|(m \times n)$ of the two-point Stokes vector have a main extremum $|S_4^{12}|(m \times n)$ and a fairly wide range of changes in random values $0.55 \div 0.75 \leq |S_4^{12}| \leq 1$ – Fig. 2 – fragments (4)–(6).

The quantitative coordinate structure of the distributions of the modulus of the fourth parameter $|S_4^{12}|(m \times n)$ of the two-point Stokes vector is characterized by the results of statistical analysis [1] – table 1.

A comparative examination of the statistical moment values presented in table 1 revealed:

- The statistical moments of higher orders, which describe the asymmetry and kurtosis of the distributions of the modulus $|SK_4^{12}|(m \times n)$ in a microscopic image of a histological section of skin dermis, are significantly higher compared to the mean and dispersion values of such distributions – $Z_{3;4}(|SK_4^{12}|) \gg Z_{1;2}(|SK_4^{12}|)$.
- The discrepancies among the values of all statistical moments $Z_{j=1;2;3;4}(|SK_4^{12}|)$ computed for varying states of polarization of the probing laser radiation are negligible, not surpassing 15%–20%.

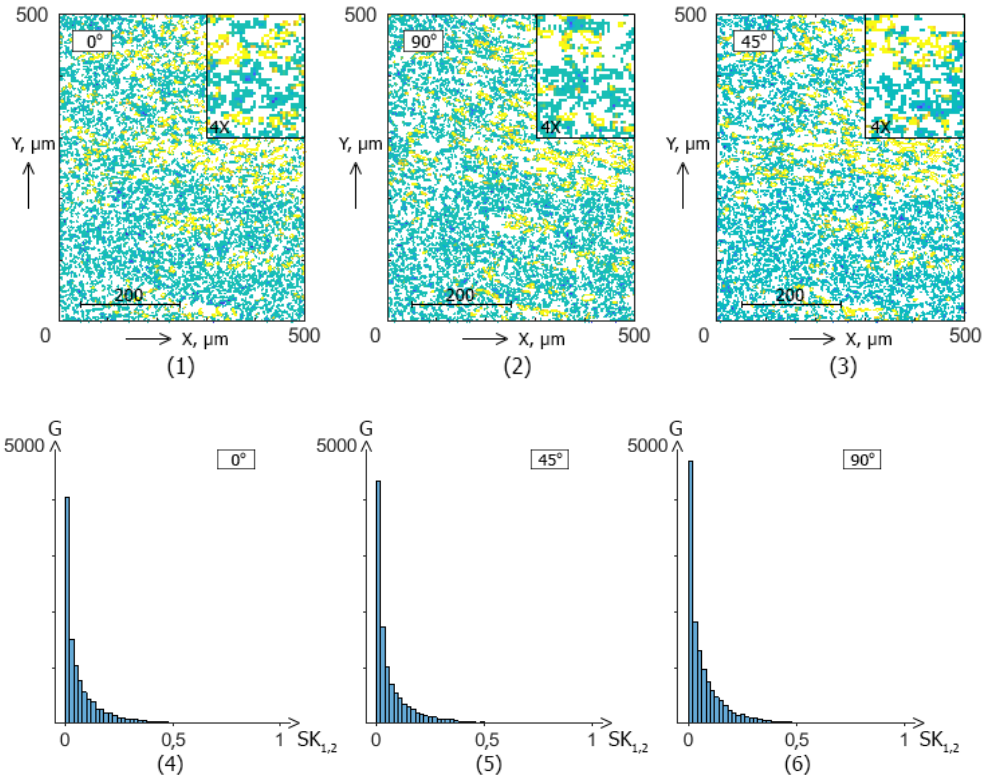

Fig. 2. Polarization-correlation maps $SK_{1,2}(m \times n)$ and histograms $G(SK_{1,2})$ of distributions $SK_{1,2}$ of a microscopic image of a histological section of the dermis of the skin for different states of polarization P of probing laser radiation

Table 1. Polarization dependences of the magnitude of statistical moments of the 1st – 4th orders characterizing the polarization-correlation maps $|SK_4^{12}|(m \times n)$ of a microscopic image of a histological section of the skin dermis

P	0^0	45^0	90^0
Z_1	0.065±0.004	0.076±0.005	0.081±0.005
Z_2	0.078±0.004	0.087±0.005	0.098±0.006
Z_3	1.83±0.11	1.67±0.09	1.51±0.08
Z_4	3.04±0.16	2.82±0.15	2.71±0.14

From a physical standpoint, the observed characteristics of polarization-correlation maps within microscopic images of histological sections of skin dermis can be linked to the predominant influence of fluctuations in random values of phase shifts (φ) between orthogonal right- and left-circular polarized components of the object laser radiation on the magnitude of the fourth parameter of the polarization-correlation vector – $|SK_4^{12}| \sim \sqrt{2\varphi_1\varphi_2}$ [14]. The sources of circular birefringence in the skin dermis are the optically active molecular domains found within the papillary layer. These domains are composed of protein molecules such as collagen and elastin. They exhibit circular birefringence and are characterized by relatively small geometric dimensions, typically ranging from approximately 2 µm to 5 µm. Moreover, these domains are randomly distributed within the volume of experimental samples of histological sections of the skin dermis. When scanning step by step $\Delta p = p_2 - p_1$ the correlation between the phase shift values of circular birefringence along a series of lines in a digital microscopic image of skin dermis histological sections is relatively low. This is primarily due to the mismatch in sizes and coordinate locations of partial optically active molecular domains, along with the deterministic linear scanning step.

The limited impact of changes in the polarization state of the irradiating laser radiation on the statistical structure of coordinate distributions of random values of the fourth parameter of the polarization-correlation vector in microscopic images of skin dermis histological sections is linked to the azimuthal symmetry observed in the arrangement of optically active molecular domains.

5. The arrangement and statistical characteristics of polarization-correlation maps specific to the spleen

In a series of segments from figure 3, the outcomes of polarization-correlation mapping are displayed for microscopic images of histological sections of spleen parenchymal tissue obtained from individuals who passed away due to myocardial infarction.

Analyzing the data obtained from polarization-correlation mapping involves examining the coordinate distributions of random values representing the modulus of the fourth parameter $|SK_4^{12}|$ analysis of the two-point Stokes vector of object fields within histological sections of spleen tissue unveiled a rise in the correlation consistency of the coordinate structure of maps $|SK_4^{12}|(m \times n)$ for microscopic images of histological sections of spleen parenchymal tissue consists of histograms depicting distributions of random values representing the modulus of the fourth parameter of the two-point Stokes vector $|SK_4^{12}|$ have a large range of variation and probability of eigenvalues that are different from zero $|SK_4^{12}| \neq 0$ – Fig. 3 – fragments (4)–(6).

Quantitative polarization-correlation maps of microscopic images of histological sections of spleen parenchymal tissue present statistical moments ranging from the 1st to the 4th orders, as detailed in table 2.

Examining the data provided in table 2 uncovered the superiority of higher-order statistical moments, which portray the asymmetry and kurtosis of distributions of random values of the quantity $|SK_4^{12}|(m \times n)$, over the eigenvalues of statistical moments of the 1st and 2nd orders. Minor differences (no more than 15%-20%) between the values of $Z_{i=1;2;3;4}(|SK_4^{12}|)$ across various states of laser irradiation polarization of samples from histological sections of spleen parenchymal tissue.

The physical analysis of the results obtained from polarization correlation mapping of microscopic images of histological sections of the spleen reveals several identified relationships. In the parenchymal architecture of spleen tissue, circular birefringence emerges as the predominant mechanism of optical anisotropy. The optically active molecular domains within the spleen stroma exhibit larger geometric dimensions and are more commonly distributed throughout the volume of experimental samples of parenchymal tissue, as opposed to the circularly birefringent protein complexes found in the papillary dermis of the skin. The parenchymal architecture of the polycrystalline component within spleen tissue contributes to a heightened degree of correlation in phase shifts between the left- and right- circularly polarized components of the object amplitude of laser radiation. As a result of the aforementioned factors, distributions of random values representing the modulus of the fourth parameter $|SK_4^{12}|$ he polarization-correlation vector of microscopic images of histological sections of the spleen exhibits significantly larger values and a wider range of variations compared to similar parameters determined for the object field of samples of fibrillar tissue in the skin dermis.

Table 2. Statistical moments of the 1st-4th orders characterizing polarization-correlation maps of a microscopic image of a histological section of the spleen

P	0^0	45^0	90^0
Z_1	0.088±0.005	0.11±0.006	0.13±0.007
Z_2	0.13±0.007	0.142±0.008	0.154±0.008
Z_3	1.48±0.08	1.57±0.09	1.38±0.07
Z_4	2.63±0.14	2.74±0.15	2.46±0.13

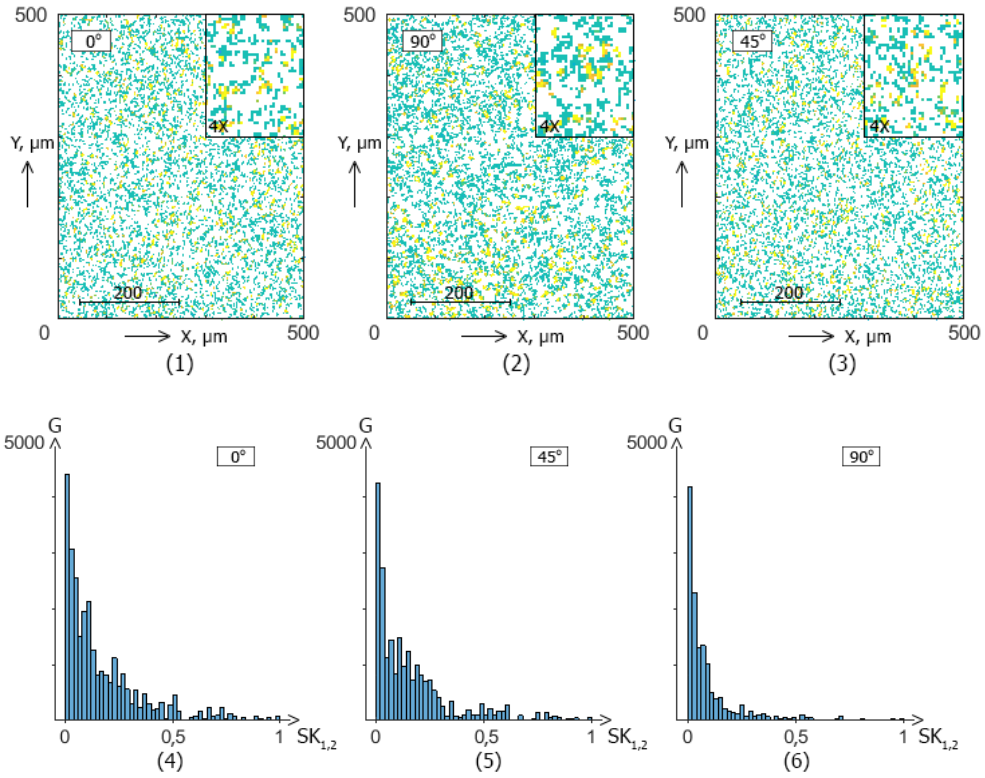

Fig. 3. Polarization-correlation maps $SK_{1,2}(m \times n)$ and histograms $G(SK_{1,2})$ of distributions $SK_{1,2}$ of a microscopic image of a histological section of the spleen for different states of polarization P

6. Conclusions

1) Mapping polarization-correlation vector maps' fourth parameter from microscopic images of histological sections of biological tissues with various architectures of the optically anisotropic polycrystalline component was conducted.
2) It has been determined that all polarization-correlation maps depicting the modulus of the fourth parameter $|S_4^{12}|(m \times n)$ of the two-point Stokes vector in microscopic images of histological sections from both skin dermis and spleen exhibit coordinated and topographically heterogeneous characteristics.
3) Through statistical analysis of the distributions of random values representing the modulus of the fourth parameter of the polarization-correlation vector in microscopic images of histological sections from fibrillar (skin dermis) and parenchymal (spleen) biological tissues, it was revealed that the values of higher-order statistical moments characterizing the asymmetry and kurtosis of the distributions of the modulus $|SK_{1,2}|(m \times n)$ in microscopic images of histological sections of both skin dermis and spleen are significantly larger compared to the mean and dispersion values of such distributions – $Z_{3;4}(|SK_{1,2}|) \gg Z_{1;2}(|SK_{1,2}|)$.
4) The disparities between the values of statistical moments of the 3rd and 4th orders are notably 2–3 times higher, suggesting their potential utility as diagnostic indicators for pathological alterations in the morphological structure of biological tissues.

Acknowledgments

Authors acknowledge the support from the Scholarship of the Verkhovna Rada of Ukraine for Young Scientists-Doctors of Science, the National Research Foundation of Ukraine.

References

[1] Ghosh N.: Tissue polarimetry: concepts, challenges, applications, and outlook. J. Biomed. Opt. 16, 2011, 110801.
[2] Jacques S. L.: Polarized light imaging of biological tissues. Boas D., Pitris C., Ramanujam N. (ed.): Handbook of Biomedical Optics 2. CRC Press, Boca Raton 2011, 649–669.
[3] Kolobrodov V. G., Nguyen Q. A., Tymchik G. S.: The problems of designing coherent spectrum analyzers. Proc. of SPIE 9066, 2013.
[4] Pavlov S. V. et al.: Electro-optical system for the automated selection of dental implants according to their colour matching. Przeglad Elektrotechniczny 93(3), 2017, 121–124,
[5] Tymchik G., Kolobrodov V. H., Mykytenko V. I.: Polarization model of thermal contrast observation objects. Thermotlectricity 1, 2020, 36–49.
[6] Tymchik G. et al.: Distortion of geometric elements in the transition from the imaginary to the real coordinate system of technological equipment. Proc. SPIE 10808, 2018, 108085C [https://doi.oeg/10.1117/12.2501624].
[7] Ushenko A. G., Pishak V. P.: Laser Polarimetry of Biological Tissues: Principles and Applications. Tuchin V. V. (ed.): Handbook of Coherent Domain Optical Methods. Springer, 2004, 93–138.
[8] Ushenko V. A., Gavrylyak M. S.: Azimuthally invariant Mueller-matrix mapping of biological tissue in differential diagnosis of mechanisms protein molecules networks anisotropy. Proc. SPIE 8812, 2016, 88120Y.
[9] Ushenko V. A. et al.: Biomedical applications of Jones-matrix tomography to polycrystalline films of biological fluids. Journal of Innovative Optical Health Sciences 12(06), 2019, 1950017.
[10] Ushenko A. et al.: Stokes-correlometry analysis of biological tissues with polycrystalline structure. IEEE Journal of Selected Topics in Quantum Electronics 25(1), 2018, 1–12.
[11] Wójcik W. et al.: Information Technology in Medical Diagnostics II. Taylor & Francis Group, CRC Press, Balkema Book, London 2019.
[12] Wójcik W. et al.: Information Technology in Medical Diagnostics. CRC Press, 2017.
[13] Wójcik W. et al.: Medical Fuzzy-Expert System for Assessment of the Degree of Anatomical Lesion of Coronary Arteries. International Journal of Environmental Research and Public Health 20(2) 2023, 979 [https://doi.org/10.3390/ijerph20020979].
[14] Zabolotna N. I. et al.: Diagnostics of pathologically changed birefringent networks by means of phase Mueller matrix tomography. Proc. SPIE 8698, 2013, 86980C.
[15] Zabolotna N. I. et al.: System of polarization phasometry of polycrystalline blood plasma networks in mammary gland pathology diagnostics. Proc. SPIE 9613, 2015, 961311.
[16] Zh Z. Z. et al.: Cluster router based on eccentricity. Eurasian Physical Technical Journal 19 (3(41)), 2022, 84–90.

Ph.D. Nataliia Kozan
e-mail: nmkozan@gmail.com

Nataliia Kozan in 1993 enrolled in studies at medical faculty of the Ivano-Frankivsk State Medical Academy, which graduated with honors in 1999. Since 2011 – associate professor, since 2019 and until today she is the head of the Department of Forensic Medicine, Medical and of Pharmaceutical Law of IFNMU. In 2005, she defended her thesis for obtaining a scientific degree Candidate of Medical Sciences, and in 2018 – Doctor of Medical Sciences by specialty 14.01.25 – forensic Medicine.

https://orcid.org/0000-0003-1017-5077

M.Sc. Oleksandr Saleha
e-mail: saleha.oleksandr@chnu.edu.ua

He is is a Ph.D. student at the Department of Optics and Publishing and Printing at Yuriy Fedkovych Chernivtsi National University Chernivtsi, Ukraine.
His research interests include laser polarimetry of optically anisotropic biological tissues and fluids of human organs.

https://orcid.org/0000-0002-0735-3920

D.Sc. Olexander Dubolazov
e-mail:.a.dubolazov@chnu.edu.ua

He is a Doctor of physics and mathematics, professor at the Department of Optics and Publishing and Printing at Yuriy Fedkovych Chernivtsi National University Cher-nivtsi, Ukraine.
His research interests include laser polarymetry and correlometry of optically aniso-tropic biological tissues and human organ fluids.

https://orcid.org/0000-0003-1051-2811

D.Sc. Yuriy Ushenko
e-mail: y.ushenko@chnu.edu.ua

He is a Doctor of physics and mathematics, professor, Head of the Department of Computer Science, Yuriy Fedkovych Chernivtsi National University Chernivtsi, Ukraine.
His research interests include Muller matrix analysis and laser polarimetry of optically anisotropic biological tissues and human organ fluids.

https://orcid.org/0000-0003-1767-1882

Ph.D. Iryna Soltys
e-mail: i.soltys@chnu.edu.ua

She is a Ph.D. in physics and mathematics, associate professor at the Department of Optics and Publishing and Printing at Yuriy Fedkovych Chernivtsi National University, Chernivtsi, Ukraine.
Her research interests include digital holography and laser polarimetry of polycrystalline facets of optically anisotropic biological fluids of human organs.

https://orcid.org/0000-0003-2156-7404

D.Sc. Oleksandr Ushenko
e-mail: o.ushenko@chnu.edu.ua

He is a Doctor of physics and mathematics, Head of the Department of Optics and Publishing and Printing at Yuriy Fedkovych Chernivtsi National University, Chernivtsi, Ukraine.
His research interests are laser polarimetry and correlometry of optically anisotropic biological tissues and fluids of human organs. Statistical, singular and fractal analysis of polarization maps and Mueller matrix images.

https://orcid.org/0009-0002-5088-592X

Ph.D. Oleksandr Olar
e-mail: cablaze9@gmail.com

He is a Ph.D. in Physics and Mathematics, associate professor at the Department of Optics and Publishing and Printing at Yuriy Fedkovych Chernivtsi National University. His research interests include digital holography and Mueller matrix laser polarimetry of polycrystalline facets of optically anisotropic biological fluids of human organs

https://orcid.org/0000-0002-3625-8439

D.Sc. Victor Paliy
e-mail: paliy@vnmu.edu.ua

He is a Doctor of medical sciences, professor at the Department of General Surgery, National Pirogov Memorial University of Vinnytsia.
Scientific direction: research of antimicrobial efficacy of a medicines with prolonged antiseptic effect and their use for treatment of purulent wounds.

https://orcid.org/0000-0002-2289-1786

Ph.D. Saule Smailova
e-mail: Saule_Smailova@mail.ru

She is a lecturer at the Department of Information Technology. D. Serikbayev East Kazakhstan State Technical University, Ust-Kamenogorsk. Member of Expert Group in the Computer Science specialization of IQAA.
Her professional interests are teaching, artificial intelligence, software engineering, data processing.

https://orcid.org/0000-0002-8411-3584